ELSEVIER

Composites Science and Technology 62 (2002) 629–639

COMPOSITES SCIENCE AND TECHNOLOGY

www.elsevier.com/locate/compscitech

Delamination identification of cross-ply graphite/epoxy composite beams using electric resistance change method

Akira Todoroki*, Yuuki Tanaka[1]

Department of Mechanical Sciences and Engineering, Tokyo Institute of Technology, 2-12-1, Ohokayama, Meguro-ku, Tokyo 1528552, Japan

Received 8 May 2001; received in revised form 17 December 2001; accepted 18 December 2001

Abstract

Detection of delaminations is a difficult task for visual inspections. Difficulty of detection underlines the importance of development of smart structures for monitoring delaminations of graphite/epoxy laminated composites. This study employs an electric resistance change method for identification of delamination location and size; applicability of the method is investigated experimentally using beam-type specimens fabricated from cross-ply laminates. On the specimen surface, multiple electrodes are mounted by co-curing copper foil to measure electric resistance changes. Interlamina shear tests are conducted to create a practical delamination crack in a beam-type specimen. Five beam specimen types were made and tested. A large number of tests were conducted to obtain a data set for solving inverse problems to estimate delamination location and size from measured electric resistance changes. Response surfaces are employed for a solver of inverse problems instead of well-known artificial neural networks. As a result, the method successfully identifies delamination location and size for these beam type specimens. To obtain practically efficient estimation performance, at least five electrodes are indispensable for these beam type specimens.

Keywords: A. Smart materials; C. Delamination; Graphite fibres

1. Introduction

Laminated composite plates fabricated by stacking unidirectional plies have superior specific mechanical properties to mechanical properties of conventional metallic materials. Laminated composite plates, however, have low delamination resistance. Low delamination resistance results in delamination cracks by slight impacts such as a tool drop. Since delamination crack creation is a serious problem for visual inspection, delamination causes low reliability for primary structure of laminated composites. To improve this low reliability, identifications of delamination cracks in-service are required. A health monitoring system to detect delamination cracks is one desirable approach for practical laminated composite structures.

One approach to identify delaminations in-service is embedding fibre-optic strain sensors into laminated composites to measure strain distributions [1–3]. This approach, however, may reduce static strength and/or fatigue strength and may increase total weight [4,5]. The approach is, moreover, very expensive due to the high cost of optical fibre sensors and the sensing system. A new technology, therefore, is desired for smart structures to identify delaminations.

The present study uses an electric-resistance change method in an attempt to identify internal delaminations experimentally. The method does not require expensive instruments. Since the method adopts reinforcing graphite fibres as sensors for delamination detections, the method does not cause static strength reduction or fatigue strength reduction, and is applicable to existing structures that have been fabricated without embedding extra sensors. Moreover, the method does not cause increased weight. Therefore, the electric-resistance change method has been adopted in several research efforts [6,7], though the method is limited to graphite fibre reinforced plastics.

Authors have already applied the electric resistance change method to measure delamination crack length for edge cracks of modes I and II tests [8]. The method was also applied to measure length of edge cracks of

* Corresponding author. Tel./fax: +81-3-5734-3178.
E-mail address: atodorok@mes.titech.ac.jp (A. Todoroki).
[1] Graduate student of Tokyo Institute of Technology.

0266-3538/02/$ - see front matter
PII: S0266-3538(02)00013-1

cross-ply and quasi-isotropic laminated composites [9]; and it was shown experimentally that the method was applicable to measure delamination crack length for laminated composites. For practical composite structures, however, delamination cracks are usually internal cracks. Through-the-width internal cracks were also detected by electric resistance change method in a previous paper using beam-type specimens with two electrodes [10]. Previous studies also conducted FEM analyses [11–13]. It was shown in Ref. [12] that identification of a delamination of a beam type specimen (estimation of delamination location and size) is impossible in cases where only a pair of electric resistance changes are measured using three electrodes mounted on the specimen surface. This is caused by strong orthotropic electric resistance. The FEM analysis also showed that electric current should be charged to fibre direction of the specimen surface. When it is charged in a transverse direction, delamination creation does not cause electric-resistance changes between electrodes [12].

In the present study, identifications of internal delaminations (estimations of delamination size and location) are attempted experimentally using beam-type cross-ply laminate specimens. Since there is a thin resin layer on the composite surfaces, it is not easy to charge electric current without electrodes. Co-cured copper foil is employed as an electrode to measure electric resistance changes precisely in the present study. Four kinds of electrode number are investigated; three, four, five, and seven. For the four-electrode specimens, two types of electrode spacing are attempted. An interlamina shear test was employed to create a delamination crack in a specimen. Electric-resistance changes between electrodes were measured using a conventional strain-gage amplifier. Response surface methodology is employed as a convenient tool to solve inverse problems to obtain delamination location and size from measured electric resistance changes.

2. Principle of electric resistance change method for delamination monitoring

Graphite fibre has a high electric conductivity and the epoxy matrix is an insulator. For ideal graphite/plastics composites, electric conductance in the fibre direction is very high. Ideal conductance can be calculated easily by multiplying fibre volume fraction by electric conductance of the graphite fibre. On the other hand, electric conductance in the transverse direction vanishes for ideal composites.

A practical graphite fibre in a unidirectional ply is serpentine as shown in Fig. 1 (a). The curved graphite fibre contacts with each other, and that makes a large graphite-fibre network in a ply. The fibre-contact-network brings non-zero electric conductance even in the transverse direction. In the same way, the fibre-network produces non-zero electric conductance in the thickness direction in a ply. Electric conductance in the transverse direction is much lower than electric conductance in the fibre direction. Authors [11] have experimentally revealed that the electric-conductance ratio of the transverse direction (σ_{90}) to the fibre direction (σ_0) is approximately $\sigma_{90}/\sigma_0 = 10^{-3}$, and that the electric conductivity ratio of the thickness direction (σ_t) to the fibre direction is approximately $\sigma_t/\sigma_0 = 10^{-4}$ for graphite/epoxy laminates.

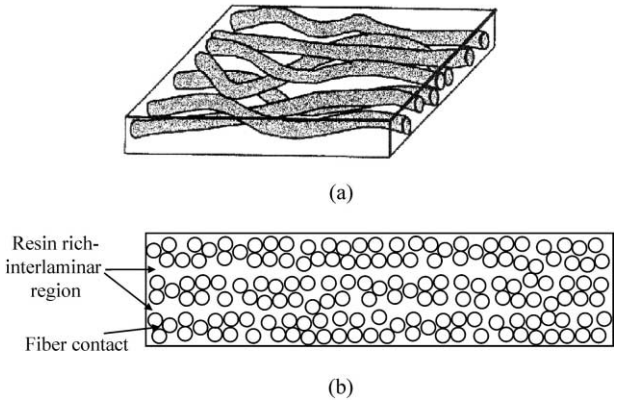

Fig. 1. Schema of practical structure of graphite/epoxy composite. (a) Network structures if fibers in a ply; (b) resin rich-interlamina region and fiber contact.

Electric conductance in the thickness direction (σ_t) is usually lower than that in the transverse direction (σ_{90}). Although fibre-network structure in the thickness direction is almost similar to that of the transverse direction in a ply, average conductance in the through-the-thickness direction (σ_t) is smaller than σ_{90} for normal laminated composites. That is owing to the fact that a thin resin rich interlamina exists and the interlamina is insulator. For ideal graphite/epoxy composites, σ_t vanishes due to the resin rich interlamina. For practical graphite/plastics composites, however, all plies are serpentine just as the fibre in a ply shown in Fig. 1(b). The ply curvature causes fibre contact through interlamina and causes non-zero electric conductance in the thickness direction even for thick laminated graphite/epoxy composites. Contact between plies causes no-zero electric conductance in the thickness direction. Thus, σ_t is usually smaller than σ_{90}. When a delamination crack grows in interlamina, the crack breaks the fibre-contact-network between plies. Breakage of the fibre-contact network causes increased electric resistance of graphite/epoxy composites. Therefore, delamination cracks can be detected by measuring electric resistance change of graphite/epoxy composite laminates.

Strong orthotropy of electric conductance causes difficulty in identification of delamination cracks. Fig. 2 shows distribution of electric current density of FEM analysis results [12] of the $[0_8]_T$ laminate at cross-section

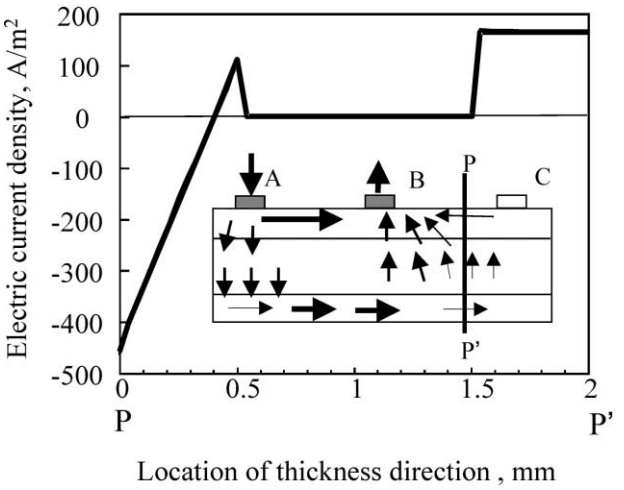

Fig. 2. FEM analysis of electric current density at the cross section P–P' when the electric current is charged between A and B (A:30 mA, B:0 V); $\sigma_{90}/\sigma_0 = 10^{-3}$ and $\sigma_t/\sigma_0 = 10^{-4}$ [11].

P–P' in the case that the electric conductivity ratio is $\sigma_t/\sigma_0 = 10^{-4}$. The ordinate is electric current density and the abscissa is the distance, in the thickness direction, from the specimen surface. Electric voltage is charged between electrodes A and B. At the cross-section of the P–P', usually there is no electric current in conventional metallic materials. However, negative electric current exists near the specimen surface. Negative current density means electric current flow of the reverse direction (from right to left). This circular flow causes electric-resistance changes even at segments between electrodes located far from a delamination. This electric-resistance change at the far segment of electrodes from delamination makes it very difficult to identify delamination location.

Fig. 3 shows results of FEM analysis of two types of stacking sequences; $[0_2/90_2]$s and $[90_2/0_2]$s [11]. The ordinate represents the electric-potential change ratio along the specimen surface and the abscissa shows distance from the charged electrode A. In the case where the stacking sequence of the laminate is $[0_2/90_2]$s (broken curve), delamination creation can cause electric-resistance change in the segment. Electric-resistance change can be obtained from difference between $\Delta V_{AB}/V^0_{AB}$ at $x = 0$ and that at $x = 140$ mm. In the case where the laminate stacking sequence is $[90_2/0_2]_T$, electric voltage change due to delamination is very large at the very point where delamination exists. Electric resistance change is, however, not measured; there is no difference between $\Delta V_{AB}/V^0_{AB}$ at $x = 0$ and that at $x = 140$ mm. This implies that delamination location identification is impossible without installing a large number of electrodes for laminates of $[90_2/0_2]_T$. Since we can afford a small limited number of electrodes for practical use, electrodes should be mounted in the fibre direction (0°-ply).

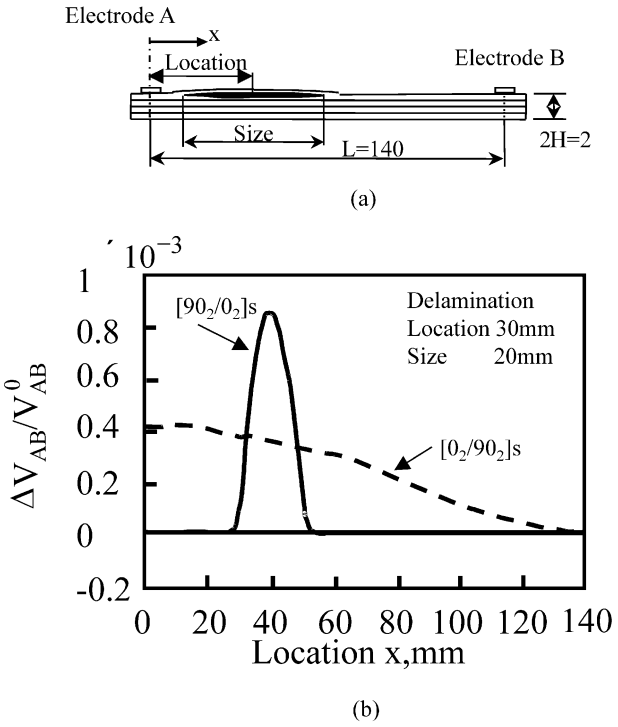

Fig. 3. Effect of stacking sequences for electric voltage change distribution after delamination creation. (a) FEM analysis model; (b) electric voltage change distribution on specimen surface by FEM analysis of cross-ply laminates.

Fig. 4 is a schematic representation of the delamination monitoring system adopted here [12]. Multiple electrodes are mounted on the specimen surface as shown in Fig. 4. All of these electrodes are placed on a single side of a specimen. Usually it is impossible to place electrodes and lead wires outside of aircraft structures. Placement of electrodes on the single side surface represents modeling of electrode placement in thin aircraft shell type aircraft structures. Electric-resistance change of each segment between electrodes is measured for various cases of delamination location and size. Using measured data, relations between electric resistance change and delamination location and size are obtained using response surfaces. After calculations for response surfaces, delamination location and size can be

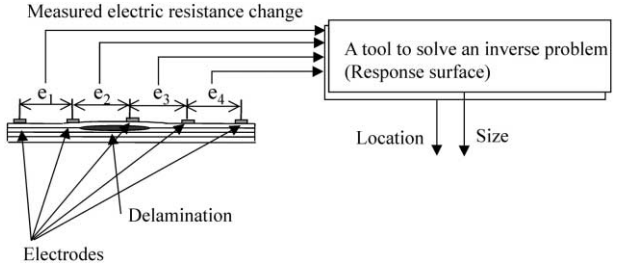

Fig. 4. Schematic representation of delamination identification method using electric resistance change method with response surfaces.

estimated with response surfaces from measured electric-resistance changes.

3. Response surface for the electric resistance change method

The response surface is a widely adopted tool for quality engineering fields [14]. Response surface methodology comprises regression curve fitting to obtain approximate responses, design of experiments to obtain minimum variances of responses, and optimizations using approximated responses.

In the present study, response surface methodology is adopted as a solution for inverse problems. For this study, predictions of delamination locations and sizes from measured electric resistance changes are one of the inverse problems. Response surface methodology brings two advantages: inverse problems can be solved approximately without consideration of modeling, and approximated response surfaces can be evaluated using powerful statistical tools. For most composites, it is very difficult to understand a precise model for electric-resistance change; and other tools like back-propagation-neural-networks present difficulties for evaluation of curve fitness.

For most of response surfaces, functions for approximations are polynomials because of their simplicity. For cases of quadratic polynomials, the response surface is described as

$$y = \beta_0 + \sum_{j=1}^{k} \beta_j x_j + \sum_{j=1}^{k} \beta_{jj} x_j^2 + \sum_{i=1}^{k-1} \sum_{j=i+1}^{k} \beta_{ij} x_i x_j \tag{1}$$

where k is the number of variables. In the case of three-electrode type specimens, there are two electric resistance change variables; v_1 and v_2. The response surface for estimations of delamination location (p) is expressed as

$$p = \beta_0 + \beta_1 v_1 + \beta_2 v_2 + \beta_3 v_1^2 + \beta_4 v_2^2 + \beta_5 v_1 v_2. \tag{2}$$

By the substitutions of $y = p, x_1 = v_1, x_2 = v_2, x_3 = v_1^2, x_4 = v_2^2, x_5 = v_1 v_2$, Eq. (2) becomes the following linear regression model.

$$y = \beta_0 + \beta_1 x_1 + \beta_2 x_2 + \beta_3 x_3 + \beta_4 x_4 + \beta_5 x_5 \tag{3}$$

In the case where total number of experiments is n, the response surface can be expressed as follows using a matrix expression:

$$\mathbf{Y} = \mathbf{X}\boldsymbol{\beta} + \mathbf{e} \tag{4}$$

where

$$\mathbf{Y} = \begin{Bmatrix} y_1 \\ y_2 \\ \vdots \\ y_n \end{Bmatrix} \mathbf{X} = \begin{bmatrix} 1 & x_{11} & x_{12} & \cdots & x_{1k} \\ 1 & x_{21} & x_{22} & \cdots & x_{2k} \\ \vdots & \vdots & \vdots & \ddots & \vdots \\ 1 & x_{n1} & x_{n2} & \cdots & x_{nk} \end{bmatrix}$$

$$\boldsymbol{\beta} = \begin{Bmatrix} \beta_0 \\ \beta_1 \\ \vdots \\ \beta_k \end{Bmatrix} \mathbf{e} = \begin{Bmatrix} \varepsilon_1 \\ \varepsilon_2 \\ \vdots \\ \varepsilon_n \end{Bmatrix}$$

where $\mathbf{e}$ is an error vector.

The unbiased estimator $\mathbf{b}$ of the coefficient vector β is obtained using the well known least square error method as follows.

$$\mathbf{b} = \left(\mathbf{X}^T\mathbf{X}\right)^{-1}\mathbf{X}^T\mathbf{Y} \tag{5}$$

The variance-covariance matrix of the $\mathbf{b}$ is obtained as

$$\mathrm{cov}\left(b_i, b_j\right) = C_{ij} = \sigma^2\left(\mathbf{X}^T\mathbf{X}\right)^{-1} \tag{6}$$

where the σ is the error of $\mathbf{Y}$. The estimated value of $\boldsymbol{\sigma}$ is obtained as

$$\sigma^2 = \frac{SS_{\mathrm{E}}}{n-k-1}. \tag{7}$$

In the previous equation, SS_{E} is a square sum of errors expressed as

$$SS_{\mathrm{E}} = \mathbf{Y}^T\mathbf{Y} - \mathbf{b}^T\mathbf{X}^T\mathbf{Y}. \tag{8}$$

In order to judge goodness of approximation of the response surface, the adjusted coefficient of multiple determination R^2_{adj} is used.

$$R^2_{\mathrm{adj}} = 1 - \frac{SS_{\mathrm{E}}/(n-k-1)}{S_{yy}/(n-1)} \tag{9}$$

In Eq. (9), S_{yy} is the total sum of squares defined in the following equation.

$$S_{yy} = \mathbf{Y}^T\mathbf{Y} - \frac{\left(\sum_{i=1}^{n} y_i\right)^2}{n} \tag{10}$$

Each coefficient of the response surface can be tested by using t-statistic. The t-statistic of coefficient b_j is expressed as

$$t_0 = \frac{b_j}{\sqrt{\sigma^2 C_{jj}}}, \tag{11}$$

where C_{jj} is the element of number jj of variance-covariance matrix of Eq. (6). When the absolute value of t-statistics is smaller than the threshold value of the t-distribution ($t_{0.025,n-k-1}$), the coefficient is eliminated from the response surface as a non-significant coefficient to obtain higher R^2_{adj}.

The response surface (RS) is a similar tool to the artificial neural network (ANN) of the famous back-propagation-training-system. The RS has advantages of easy calculation and availability of strong statistical tools in compensation for decreased fitness compared to the ANN. Our previous paper shows that the RS gives enough approximations for the inverse tool of electric-resistance change method for delamination monitoring of graphite/epoxy laminates [12]; and the ANN may give larger error for new data that are not used for training. On the other hand, RS gives better estimations even for new data. On the basis of the results, RS is adopted here.

4. Specimens and experimental procedures

4.1. Specimens

Material used in the present paper is unidirectional graphite/epoxy prepreg. The type of the unidirectional prepreg sheet is A125-Rc33% produced by Shin-Nihon Steel Chemistry Co. The stacking sequence is $[0_2/90_2]$s, and thickness is approximately $t = 1$ mm. Cure condition is 180 °C×1 MPa×2 h. To measure electric-resistance changes between electrodes using a two-probe method, reliable electrodes are indispensable. To make reliable electrodes, rectangle copper foil of 0.02 mm thickness is mounted on prepreg laminates; and these electrodes are then co-cured with the laminate. Several types of beam specimens of 15 mm width are made from laminated plates.

In order to examine the effect of number of electrodes and size of spacing between electrodes, five types of beam specimens were prepared. These specimen configurations are shown in Fig. 5. For each type of specimen in the present study, multiple electrodes are mounted on a single surface of the specimen. The reason for placement of all electrodes on the same surface is to simulate identification of an invisible internal delamination crack by mounting electrodes on the inner surface of a shell-type structure such as an aircraft. The type A specimen has three electrodes with length of 180 mm spaced at 90 mm. The type B specimen has four electrodes with length of 180 mm spaced at 60 mm. The type C specimen has four electrodes with length of 135 mm spaced at 45 mm. The type D specimen has five electrodes with length of 180 mm spaced at 45 mm. The type E specimen has seven electrodes with length of 270 mm spaced at 45 mm.

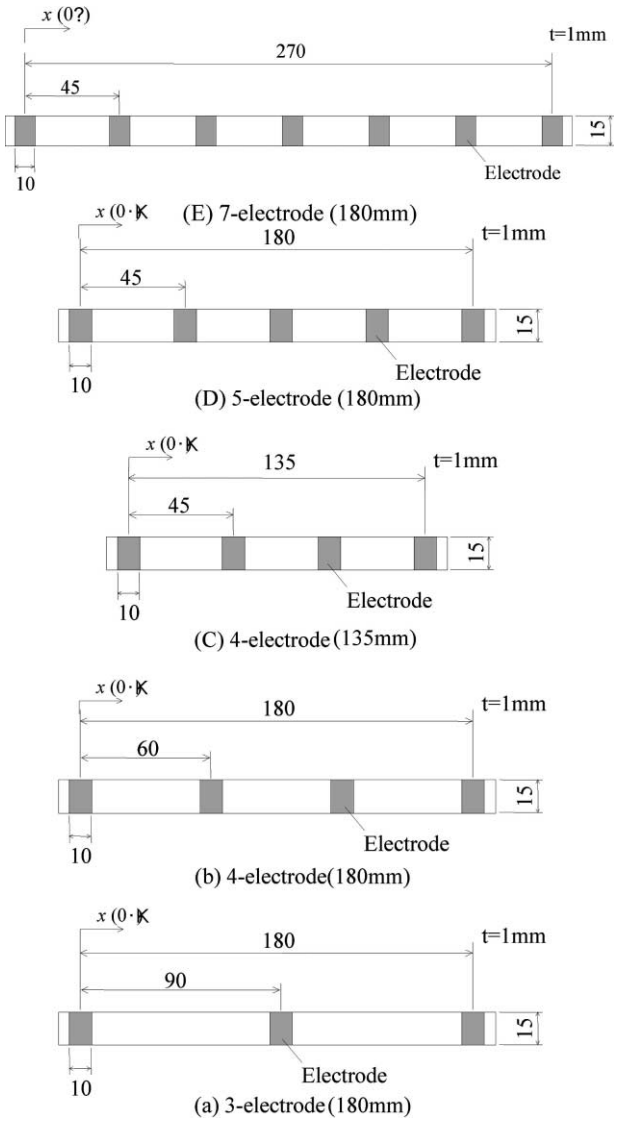

Fig. 5. Specimen configurations.

4.2. Electric circuit

Since electric-resistance change due to delamination crack creation is very small, electric-resistance change is measured with the electric-resistance bridge circuit as shown in Fig. 6. As easily recognized, the bridge circuit is similar to that of conventional strain gages. Therefore, conventional strain-gage amplifiers are adopted for measurement of electric resistance change of specimens. That causes labeling of instrument output as "strain", but it does not imply specimen deformation. The output "strain" means electric-resistance change ratio. The electric-resistance change ratio is expressed using output "strain" data ε shown as

$$\frac{\Delta R}{R} = k\varepsilon \tag{14}$$

where ΔR is the electric-resistance change due to creation of a delamination crack, R is initial electric resistance, k is a gage factor, and ε is the output "strain". Usually, the gage factor adopted for the conventional strain-gage amplifier is two. To obtain higher output "strain" data, the electric-resistance change ratio $\Delta R/R$ should be large. Since the electric-resistance change (ΔR) is very small and the measured initial electric resistance (R) of the specimen is approximately 0.8Ω , the electric resistances of the bridge circuit are arranged from the normal circuit for conventional strain gages. By trial and error, electric resistance of 3 Ω is selected as initial resistance R in this bridge circuit. Electric resistance of 240 Ω is also connected to the bridge circuit to prevent charging a large electric current. Since measured output is ε, ε is called the electric-resistance change ($v = \Delta R/R/k$) in the present study though it still includes the effect of the gage factor.

4.3. Experimental procedures

To create a delamination crack in each beam-type specimen, an interlamina-shear test is employed here. The middle point is loaded from the opposite side of electrode mountings. This is to simulate electrode placement inside structures and to simulate the condition in which impact load comes from the exterior. Since the specimen is a thin laminate, loading creates a large delamination crack in the 0°–90° interface near the electrodes. This test method is shown schematically in Fig. 7.

After creating a delamination crack, electric-resistance changes of all segments between electrodes were measured using a conventional strain-amplifier. Delamination location and size (length) were measured using an ultrasonic C-scan image. The delamination location is decided at the center point of the delamination crack from the specimen end. Delamination size (length) is defined as maximum length of delamination in the longitudinal direction. For the three-electrode type specimen (Type A), measured electric resistances are v_1 and v_2. For the seven-electrode type specimen (Type E), measured electric resistance changes are v_1, v_2, v_3, v_4, v_5, and v_6 for example. The total number of experiments for each type of specimen is shown in Table 1.

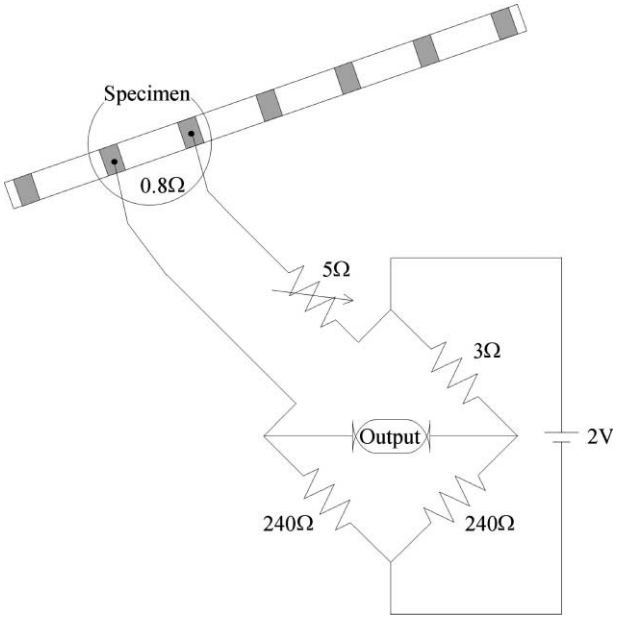

Fig. 6. Electric resistance bridge circuit employed in the present study.

5. Experimental results and discussion

5.1. Measured electric resistance changes

Results of measured electric-resistance change ($v = \Delta R/R/k$) reveal that co-cured electrodes are reliable enough and that the inverse problem to estimate delamination locations and size from measured electric-resistance changes is a difficult problem. Typical measured electric-resistance changes of the type A specimen (three-electrode) are shown in Fig. 8. The ordinate is measured electric-resistance change and the abscissa is the segment number between electrodes. The output electric-resistance changes themselves are large enough for practical measurements. In Fig. 8, results for two specimens are shown. Both specimens have similar delaminations: locations are 110.8 and 115.1 mm, and sizes are 6.7 and 5.2 mm respectively. Approximate delamination location is shown in the figure with a black arrow. Although the two experiments have similar delamination cracks, measured electric-resistance

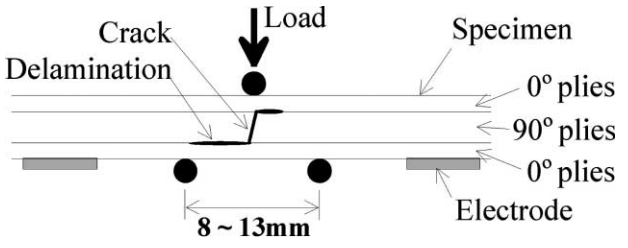

Fig. 7. Method for delamination creation.

Table 1
Numer of experiments conducted in each specimen

Type (number of electrodes)	Number of experiments
A (3)	23
B (4)	19
C (4)	15
D (5)	20
E (7)	51

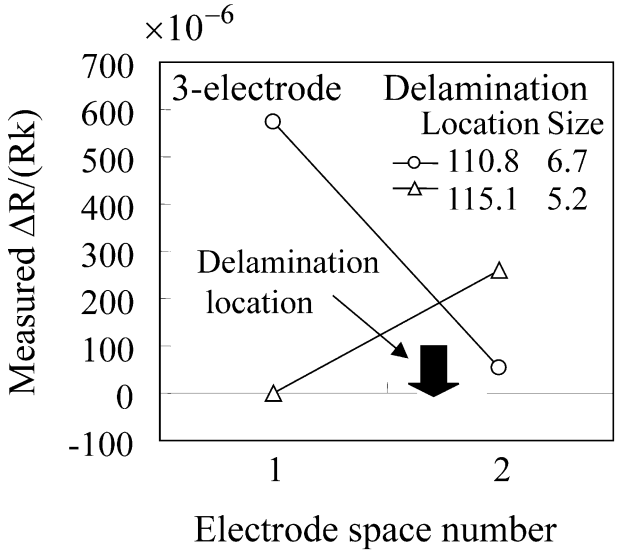

Fig. 8. Measured electric resistance of type A specimen; two results of specimens that have similar delamination with each other.

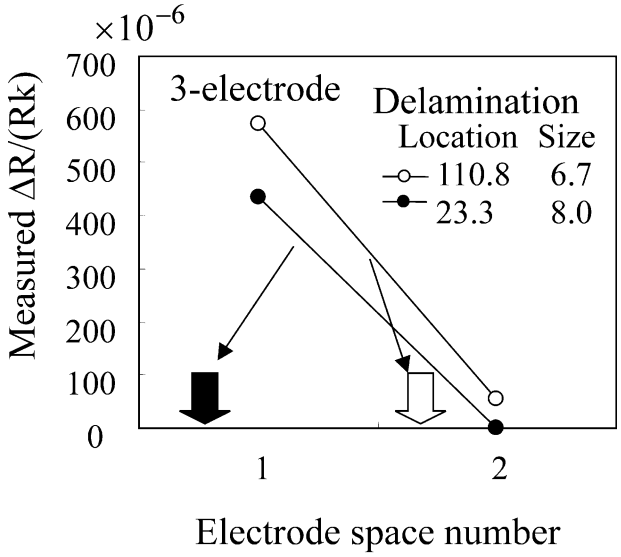

Fig. 9. Measured electric resistance of type A specimen; two results of specimens that have different delamination but have similar results.

changes are completely different from one another. Fig. 9 shows results for other specimens. In this case, delamination locations of the two specimens are different from one another. Open symbols are results of location at 110.8 mm and solid symbols are results of location at 23.3 mm. These two results, however, have similar distributions of electric-resistance changes. Similar results are obtained in type E specimens. Fig. 10 shows results of measured electric resistance change of type E specimens. In the figure, the black arrow shows the approximate location of delamination. The segment that provides the maximum result does not always equal the segment where delamination exists. The complicated results imply that the inverse problem to estimate delamination locations is not a simple quiz.

Since experimental error owing to electric noise for measurements is approximately less than 10×10^{-6}, the reason why measured electric-resistance changes are so complicated is inferred to be the contribution of delamination transitions and a matrix cracking created at the same time of the creation of the delamination. Fig. 11 shows two typical results for type E specimens. Both specimens have delamination cracks of similar sizes and locations except for the matrix crack and delamination location in the thickness directions. Results represented by solid symbols have a delamination configuration similar to the letter "Z". This configuration is called a Z-type configuration delamination crack here. The delamination crack transits from the upper 0°–90° interface to lower 0°–90° interface with a matrix crack in the inner 90° plies. On the other hand, the delamination crack represented by the open symbols transits from the lower interface to the upper interface in a reversed Z-type configuration. These results for the two types differ with one another. These delamination crack configuration differences in the thickness direction have significant effect on measured electric-resistance change. This delamination-transition effect due to a matrix crack is inferred to cause difficulty in delamination crack location estimates.

5.2. Performance of estimations and the effect of number of electrodes

Using measured experimental data, response surfaces for estimating delamination locations and size were created with the least square error method and estimations of delamination location and size were conducted. Estimation results for delamination locations of all types (from three-electrodes to seven electrodes) are shown in Fig. 12: Fig. 12(a) shows results of the type A (three-electrode) specimens; Fig. 12(b) shows results of type B specimens (wide-spacing-four-electrode); Fig. 12(c) shows results of the type C (narrow-spacing four-electrode); Fig. 12(d) shows results of the type D (five-electrode) specimens; and Fig. 12(e) shows results of the type E (seven-electrode) specimens. For all figures, ordinates are estimated delamination locations and abscissas are measured delamination locations. Symbols placed on diagonal lines mean that response surfaces provide exact estimations. Table 2 provides the set of R^2_{adj} of response surfaces for estimations of delamination locations.

All of these figures and a table imply that performance for delamination locations estimations is improved with increased of the number of electrodes. For cases of type A, B, and C (three-electrode and four-electrode), response surfaces give relatively poor performance and lower values of R^2_{adj}. When the number of

electrodes is higher than five, performance of estimations of response surfaces becomes excellent. To qualify performance of delamination location estimations, allowable error of estimations is set to 25 mm (approximately half the electrode spacing), and practical performance of estimation is counted for estimation results of experimental data. Broken lines in the figures represent error bands of 25 mm. The number of estimations located within error bands is counted and that number is divided by the total number of experiments to obtain practical performance of the delamination location estimations. Results are shown in Fig. 13 with triangle symbols. Obviously, practical performance is improved with increased electrode number. When the practical allowable threshold is set to 95% reliability for practical performance, the minimum required number of electrodes is five. This result agrees well with the analytical result obtained in our previous paper [12].

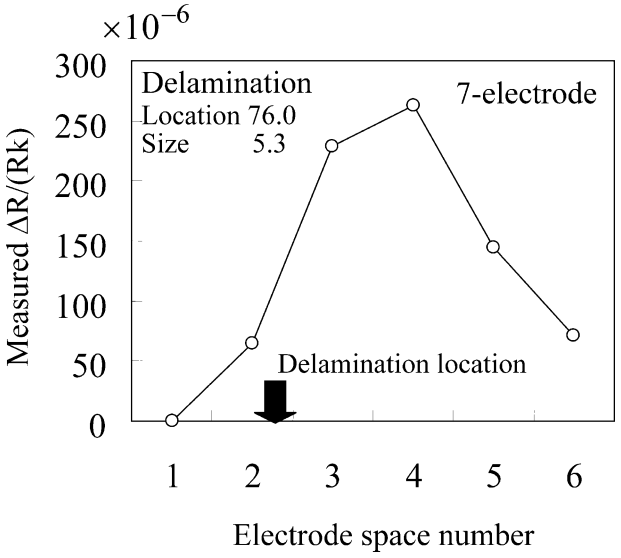

Fig. 10. Measured electric resistance of type E specimen.

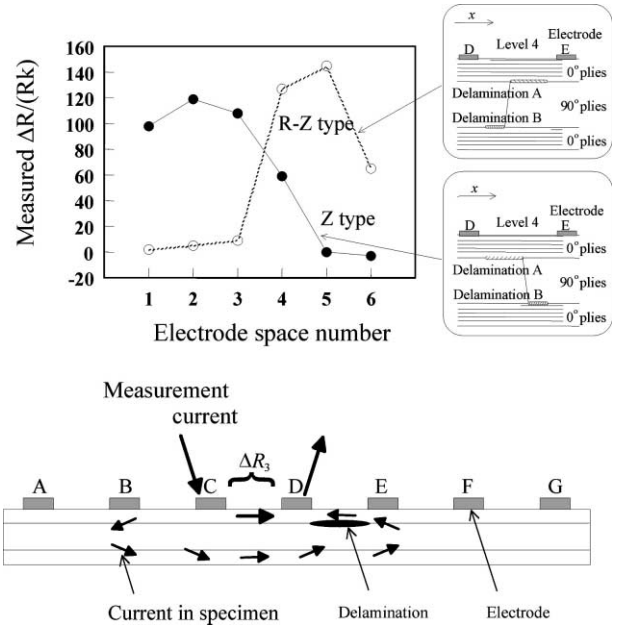

Fig. 11. Measured electric resistance of type E specimen; two results of specimens that have similar delaminations but have different results.

Effect of the size of spacing between electrodes is shown in type B and C results. Type B is the wide-spaced four-electrode type specimen (60 mm) and type C is the narrow-spaced four-electrode type specimen (45 mm). Comparing type B results with type C results, it is clear that there is little difference in estimation performance. Narrow spacing does not cause significant increase of estimation performance. At least, this implies that electrode spacing is not so significant compared to the effect of electrode number for this type of specimen.

Fig. 14 shows estimates of delamination size (delamination length in the longitudinal direction) for all types of specimens. As in Fig. 12, results from types A–E are shown in (a)–(e) respectively. Results of R^2_{adj} of all response surfaces for estimations of delamination sizes are shown in Table 3. For delamination size estimations, values of R^2_{adj} are all sufficiently high except for type A. The result shows that estimation of size is not a difficult problem. The same result is also obtained using FEM analyses in our previous paper [12].

Since the C-scan ultrasonic image method itself has error of approximately 2 mm for measurements of delamination size, practical allowable error for delamination size estimates is set to 3 mm to obtain practical estimation performance. Broken lines in figs. show error bands. Practical performances for all types are calculated as described before. Results are shown in Fig. 11

Table 2
R^2_{adj} of response surface for estimations of delamination location

Type (number of electrodes)	R^2_{adj} (%)
A (3)	40.9
B (4)	31.0
C (4)	31.0
D (5)	89.0
E (7)	93.2

Table 3
R^2_{adj} of response surface for estimations of delamination size (length)

Type (number of electrodes)	R^2_{adj} (%)
A (3)	57.6
B (4)	72.6
C (4)	72.6
D (5)	87.0
E (7)	76.6

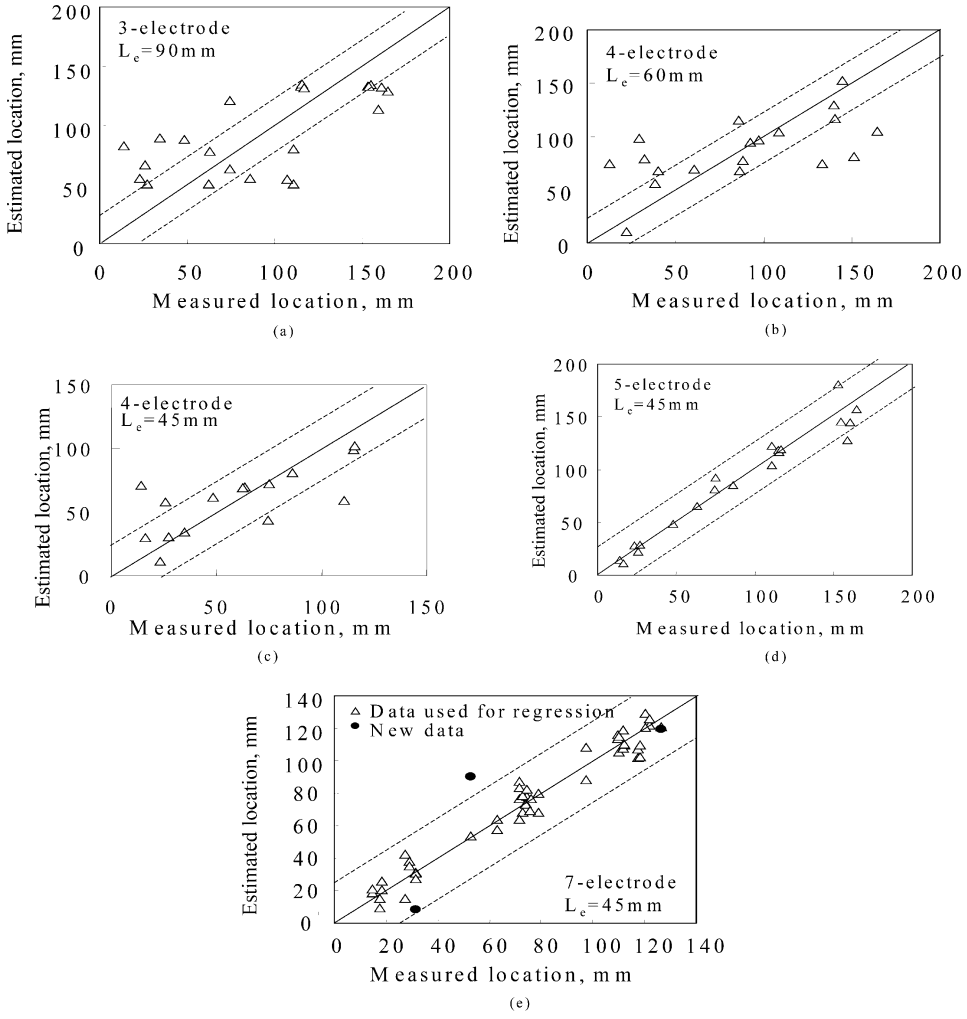

Fig. 12. Estimation of delamination locations. (a) type A, (b) type B, (c) type C, (d) type D, (e) Type E.

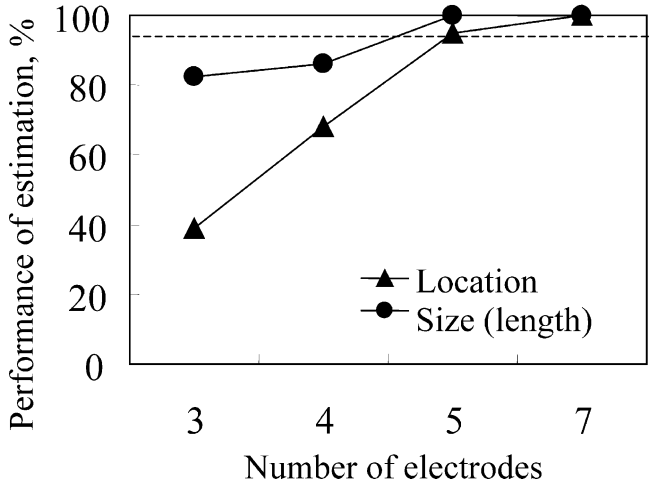

Fig. 13. Effect of the number of electrodes on the practical performance of estimations of location and size.

with circle symbols. Even in this case, the required number of electrodes to obtain practical performance of 95% is five. From these results, it can be concluded that more than five electrodes should be mounted on the specimen to identify delamination location and size for beam-type specimens.

Solid symbols in Figs. 12(e) and 14(e) are estimation results for new data that are not used for regressions to

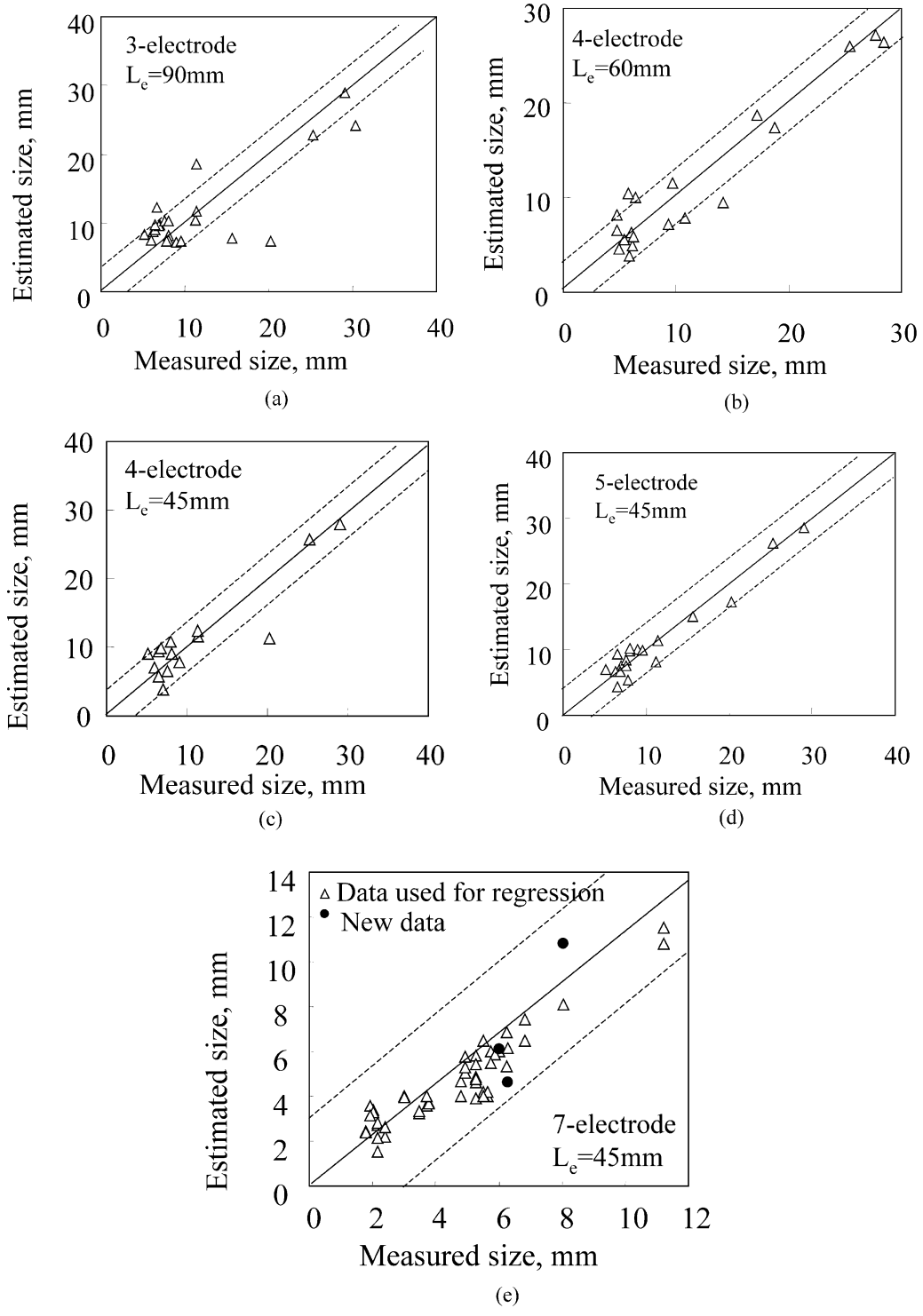

Fig. 14. Estimation of delamination sizes (length). (a) type A, (b) type B, (c) type C, (d) type D, (e) type E.

calculate response surfaces. These solid symbols locate close to diagonal lines in these figures. This means that estimation of the response surface is closely approximate even for new data. From these results, we can conclude that the electric-resistance-change method is applicable for delamination identification.

6. Conclusions

This present study investigates, experimentally and in detail, delamination identification of graphite/epoxy composites using electric resistance change with response surfaces. Results are as follows.

(1) Delamination identifications of graphite/epoxy laminated composites are successfully conducted with the electric-resistance change method using response surfaces.

(2) In order to obtain practically acceptable identification performance, at least five electrodes are required for beam type specimens. Electrode number has more significant effect on the identifications than spacing of electrodes.

(3) Electric-resistance changes due to delamination creation can be measured with multiple co-cured electrodes mounted on a single surface of a beam type specimen.

References

1 Badcock RA, Franklyn G. Fernando, an intensity-based optical fibre sensor for fatigue damage detection in advanced fibre-reinforced composites. Smart Materials and Structures 1995;4:223–30.

2 Chang CC, Sirkis JS. Impact-induced damage of laminated graphite/epoxy composites monitoring using embedded in-line fiber etalon optic sensors. Journal of Intelligent Material Systems and Structures 1997;8:829–41.

3 Chang CC, Sirkis JS. Design of fiber optic sensor systems for low velocity impact detection. Smart Materials and Structures 1998;7:166–77.

4 Seo DC, Lee JJ. Effect of embedded optical fiber sensors on transverse crack spacing of smart composite structures. Composite Structures 1995;32:51–8.

5 Lee DC, Lee JJ, Yun S-J. The mechanical characteristics of smart composite structures with embedded optical fiber sensors. Composite Structures 1995;32:39–50.

6 Irving PE, Thiagarajan C. Fatigue damage characterization in graphite fibre composite materials using an electric potential technique. Smart Materials and Structures 1998;7:456–66.

7 Abry JC, Bochard S, Chateauminois A, Salvia M, Giraud G. In situ monitoring of flexural fatigue damage in CFRP laminates by electric resistance measurements. Proceedings of 4th ESSM and 2nd MIMR conference, Harrogate, 1998. p. 389–96.

8 Todoroki A, Matsuura K, Kobayashi H. Application of electric potential method to smart composite structures for detecting delamination. JSME International J, Series A 1995;38(4):524–30.

9 Todoroki A, Kobayashi H, Matsuura K. Application of electrical potential method as delamination sensor for smart structures of graphite/epoxy. In: Inoue K, Shen SIY, Taya M, editors. US-Japan Workshop on Smart Materials and Structures, University of Washington TMS, 1997. p. 47–54.

10 Todoroki A. Delamination detection by electric resistance change for graphite/peek composites. In: Proceedings of the 5th Japan International SAMPE Symposium, 1997. p. 899–904.

11 Todoroki A, Suzuki H. Evaluation of orthotropic electrical resistance for delamination smart detection of graphite/epoxy composites by electrical potential method. In: Proceedings of 1st Asian–Australian Conference on Composite Materials (ACCM-1), 1998. p. 630–1–630–4.

12 Todoroki A, Suzuki H. Health monitoring of internal delamination cracks for graphite/epoxy by electric potential method. Applied Mechanics and Engineering 2000;5(1):283–94.

13 Todoroki A. Effect of number of electrodes and diagnostic tool for delamination monitoring of graphite/epoxy laminates using electric resistance change. Composite Science and Technology 2001;61(13):1871–80.

14 Myers RH, Montgomery DC. Response surface methodology: process and poduct optimization using designed experiments. New York: John Wiley & Sons Inc, 1995.